Valence-electron configuration of Fe, Cr, and Ni in binary and ternary alloys from $K\beta$-to-$K\alpha$ x-ray intensity ratios

I. Han[1,*] and L. Demir[2]
[1]*Faculty of Arts and Sciences, Department of Physics, Ağrı İbrahim Çeçen University, 04100 Ağrı, Turkey*
[2]*Faculty of Sciences, Department of Physics, Atatürk University, 25240 Erzurum, Turkey*
(Received 21 July 2009; published 10 November 2009)

$K\beta$-to-$K\alpha$ x-ray intensity ratios of Fe, Cr, and Ni have been measured in pure metals and in alloys of Fe_xNi_{1-x} (x=0.8, 0.7, 0.6, 0.5, 0.4, 0.3, and 0.2), Ni_xCr_{1-x} (x=0.8, 0.6, 0.5, 0.4, and 0.2), Fe_xCr_{1-x} (x=0.9, 0.7, and 0.5), and $Fe_xCr_yNi_{1-(x+y)}$ (x=0.7−y=0.1, x=0.5−y=0.2, x=0.4−y=0.3, x=0.3−y=0.3, x=0.2−y=0.2, and x=0.1−y=0.2) following excitation by 22.69 keV x rays from a 10 mCi ^{109}Cd radioactive point source. The valence-electron configurations of these metals were determined by corporation of measured $K\beta$-to-$K\alpha$ x-ray intensity ratios with the results of multiconfiguration Dirac-Fock calculation for various valence-electron configurations. Valence-electron configurations of 3d transition metals in alloys indicate significant differences with respect to the pure metals. Our analysis indicates that these differences arise from delocalization and/or charge transfer phenomena in alloys. Namely, the observed change of the valence-electron configurations of metals in alloys can be explained with the transfer of 3d electrons from one element to the other element and/or the rearrangement of electrons between 3d and 4s,4p states of individual metal atoms.

DOI: 10.1103/PhysRevA.80.052503 PACS number(s): 32.30.Rj, 32.70.Fw

I. INTRODUCTION

The variety of physical properties of the 3d transition metals and the large number of applications of these metals and their compounds and alloys cause the need for understanding the valence-electron configurations of 3d transition metals in various systems. This stimulates the development of experimental and theoretical methods to investigate the influence of chemical and/or solid state effects on valence-electron structure of 3d transition metals. The $K\beta$-to-$K\alpha$ x-ray intensity ratios of 3d transition metals depend on the chemical environment of these metals in their alloys [1–7] and compounds [8–20]. This dependence can be explained as the result of the changes of the 3d electron population of the transition metal because of chemical and/or solid state effects, which modify 3p orbitals more than 2p orbitals resulting in a change in the $K\beta$-to-$K\alpha$ x-ray intensity ratio of the metal. Thus the $K\beta$-to-$K\alpha$ x-ray intensity ratio becomes a sensitive tool to study the valence-electron configurations of the 3d-transition metals in various systems.

Comparison of the experimental $K\beta$-to-$K\alpha$ x-ray intensity ratio values with the theoretical values obtained from the multiconfiguration Dirac-Fock (MCDF) calculations for various valence-electron configurations is a convenient method to determine the valence-electron configurations of the 3d-transition metals in alloys and compounds. This method was worked out and tested for the valence-electron configuration of various 3d-transition metals in some earlier works [21–23]. The MCDF method that has been mainly developed by Grant and co-workers is described in detail [24–31].

The present experimental study is on valence-electron configuration of Fe, Cr, and Ni in binary and ternary alloys from $K\beta$-to-$K\alpha$ x-ray intensity ratios and has two-sided aspect. The main goal of this study is related to the estimation (by the comparison of the experimental $K\beta$-to-$K\alpha$ x-ray intensity ratio values with the theoretical ones obtained by MCDF calculations) of the numbers of 3d and 4s,4p electrons for metals in an alloy. In this way obtained valence-electron structure of a given metal in an alloy is found to be different from that of pure metal. This difference was explained with the charge transfer and electron rearrangement processes. Results of this part show that $K\beta$-to-$K\alpha$ x-ray intensity ratios are a useful and sensitive physical quantity to determine the valence-electron configurations of the 3d transition metals.

The second aim of this study is to estimate the average number of 3d and 4s,4p electrons for alloy. Obtained average valence-electron configuration of an alloy differs from superposition of the configuration of pure metals constituting

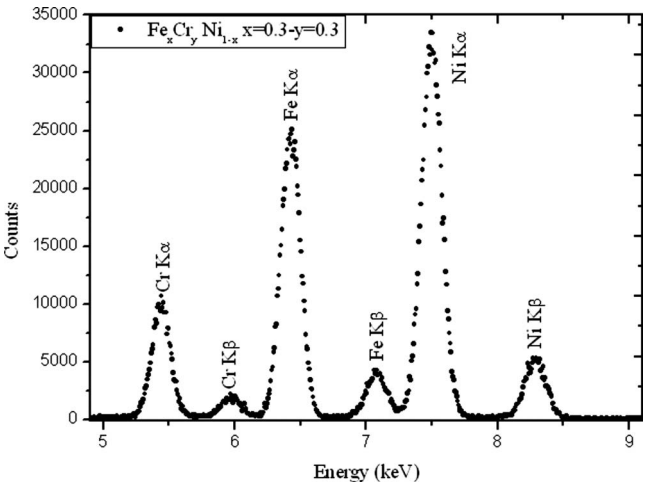

FIG. 1. A typical K x-ray spectrum of $Fe_{0.3}Cr_{0.3}Ni_{0.4}$ alloy.

*Corresponding author. FAX: +90 4422360948; ibrahimhan25@hotmail.com

TABLE I. $K\beta$-to-$K\alpha$ x-ray intensity ratios of Fe, Cr, and Ni in pure metals and different alloys ($N_{K\beta}/N_{K\alpha}$: before correction, $I_{K\beta}/I_{K\alpha}$: after correction, and $R_{K\beta}/R_{K\alpha}$: normalized $K\beta$-to-$K\alpha$ x-ray intensity ratios with respect to the pure metals).

	Fe			Cr			Ni		
Sample	$N_{K\beta}/N_{K\alpha}$	$I_{K\beta}/I_{K\alpha}$	$R_{K\beta}/R_{K\alpha}$	$N_{K\beta}/N_{K\alpha}$	$I_{K\beta}/I_{K\alpha}$	$R_{K\beta}/R_{K\alpha}$	$N_{K\beta}/N_{K\alpha}$	$I_{K\beta}/I_{K\alpha}$	$R_{K\beta}/R_{K\alpha}$
Pure Fe	0.1488	0.1320	1.0000						
Pure Cr				0.1442	0.1273	1.0000			
Pure Ni							0.1488	0.1333	1.0000
$Fe_{0.8}Ni_{0.2}$	0.1607	0.1284	0.9778				0.1778	0.1369	1.0361
$Fe_{0.7}Ni_{0.3}$	0.1615	0.1290	0.9826				0.1763	0.1365	1.0326
$Fe_{0.6}Ni_{0.4}$	0.1632	0.1303	0.9927				0.1742	0.1350	1.0215
$Fe_{0.5}Ni_{0.5}$	0.1645	0.1313	0.9997				0.1743	0.1353	1.0239
$Fe_{0.4}Ni_{0.6}$	0.1669	0.1332	1.0147				0.1722	0.1347	1.0194
$Fe_{0.3}Ni_{0.7}$	0.1677	0.1338	1.0190				0.1695	0.1339	1.0128
$Fe_{0.2}Ni_{0.8}$	0.1691	0.1350	1.0283				0.1643	0.1311	0.9916
$Fe_{0.9}Cr_{0.1}$	0.1597	0.1309	0.9922	0.1724	0.1327	1.0427			
$Fe_{0.7}Cr_{0.3}$	0.1602	0.1317	0.9988	0.1722	0.1294	1.0168			
$Fe_{0.5}Cr_{0.5}$	0.1644	0.1326	1.0050	0.1651	0.1265	0.9940			
$Cr_{0.2}Ni_{0.8}$				0.1667	0.1291	0.9847	0.1678	0.1300	0.9848
$Cr_{0.4}Ni_{0.6}$				0.1678	0.1301	0.9924	0.1786	0.1332	1.0076
$Cr_{0.5}Ni_{0.5}$				0.1712	0.1323	1.0076	0.1839	0.1353	1.0227
$Cr_{0.6}Ni_{0.4}$				0.1735	0.1344	1.0229	0.1889	0.1371	1.0379
$Cr_{0.8}Ni_{0.2}$				0.1786	0.1383	1.0534	0.2006	0.1444	1.0909
$Fe_{0.7}Cr_{0.1}Ni_{0.2}$	0.1503	0.1309	0.9915	0.1488	0.1317	1.0348	0.1647	0.1364	1.0231
$Fe_{0.5}Cr_{0.2}Ni_{0.3}$	0.1530	0.1317	0.9976	0.1454	0.1284	1.0089	0.1632	0.1345	1.0088
$Fe_{0.4}Cr_{0.3}Ni_{0.3}$	0.1540	0.1316	0.9972	0.1429	0.1265	0.9940	0.1632	0.1328	0.9962
$Fe_{0.3}Cr_{0.3}Ni_{0.4}$	0.1546	0.1325	1.0041	0.1444	0.1271	0.9983	0.1632	0.1332	0.9993
$Fe_{0.2}Cr_{0.2}Ni_{0.6}$	0.1556	0.1344	1.0182	0.1452	0.1278	1.0039	0.1606	0.1330	0.9978
$Fe_{0.1}Cr_{0.2}Ni_{0.7}$	0.1597	0.1376	1.0428	0.1467	0.1290	1.0134	0.1594	0.1321	0.9910

this alloy. This originates from the changes of valence-electron configuration of individual metals in alloys.

II. EXPERIMENTAL DETAILS, DATA ANALYSIS, AND CORRECTIONS

The measurements were carried out using high purity alloys (in powder form). The powder material is pelletized into the size of 13 mm diameter. The samples were irradiated using 22.69 keV x rays from a 10 mCi ^{109}Cd radioactive point source. For each sample, emitted x rays were detected by a Si(Li) detector (full width at half maximum=160 eV for a 5.9 keV x-ray peak, active area of 12 mm^2, thickness of 3 mm, and Be window thickness of 0.025 mm) coupled with a multichannel analyzer system and spectroscopy amplifier. The detector was also placed in a step-down shield made from Pb, Fe, and Al to minimize the detection of any radiation coming directly from the source and scattered from the surroundings.

A typical K x-ray spectrum of $Fe_{0.3}Cr_{0.3}Ni_{0.4}$ alloy is shown in Fig. 1. All the x-ray spectra were carefully analyzed by means of the Microcal Origin 7.5 Demo Version software program using a multi-Gaussian least-squares fit method in order to determine the net peak. The $K\beta$-to-$K\alpha$ intensity ratios were determined from peak areas fitted to Gaussian function after applying necessary corrections to the data. For measured ratios corrections are needed because of the difference in the $K\alpha$ and $K\beta$ self-attenuations in the sample, difference in the efficiency of the Si(Li) detector and air absorption on the path between the sample and the Si(Li) detector window. Details regarding the data analysis, correction, and calculation procedures for $K\beta$-to-$K\alpha$ x-ray intensity ratios have been reported in our previous papers [32,33].

To estimate the self-attenuation correction in the sample and the absorption correction in the air path, we used the mass attenuation coefficients obtained by means of a computer program named WINXCOM [34,35]. This program uses mixture rule to calculate the partial and total mass attenuation coefficients for all elements, compounds, and mixtures

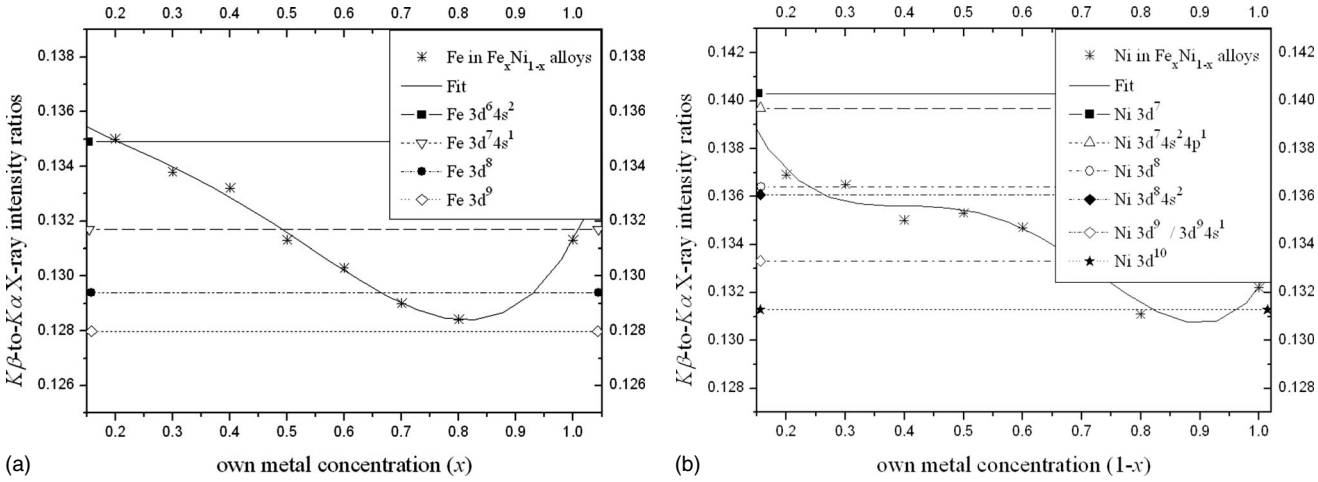

FIG. 2. Comparison of the experimental $K\beta$-to-$K\alpha$ x-ray intensity ratios for Fe and Ni in Fe_xNi_{1-x} alloys with the results of MCDF calculations for different valence-electron configuration of Fe and Ni.

at standard as well as selected energies. The mass attenuation coefficients $(\mu/\rho)_C$ for any chemical compound or mixture are estimated using the elemental values in the following Bragg-rule formula [36]:

$$(\mu/\rho)_C = \sum_i w_i(\mu/\rho)_i,$$

where w_i is the proportion by weight of the ith constituent and $(\mu/\rho)_i$ is the mass attenuation coefficient for the ith constituent in the compound.

The efficiency of the detector may be estimated theoretically using the following expression [2]:

$$\varepsilon_d(E_x) = e^{-(\mu_{Be}x_{Be}+\mu_{Au}x_{Au}+\mu_{Si}\Delta x_{Si})}(1-e^{-\mu_{Si}x_{Si}}),$$

where μ_{Be}, μ_{Au}, and μ_{Si} are absorption coefficients of the Be window of the Si(Li) detector, the Au layer on the Si(Li) crystal, and the Si(Li) crystal for detected x rays of energy E_x, respectively. x_{Be}, x_{Au}, and x_{Si} are the thicknesses of the Be window, the Au layer, and the Si(Li) crystal, respectively. The Δx_{Si} is thickness of insensitive region of the Si(Li) crystal.

III. RESULTS AND DISCUSSION

Uncorrected, corrected, and normalized results of measured $K\beta$-to-$K\alpha$ x-ray intensity ratios of Fe, Cr, and Ni in pure metals and their different alloy compositions (for Fe_xNi_{1-x}, x=0.8, 0.7, 0.6, 0.5, 0.4, 0.3, and 0.2, for Ni_xCr_{1-x}, x=0.8, 0.6, 0.5, 0.4, and 0.2, for Fe_xCr_{1-x}, x=0.9, 0.7, and 0.5, and for $Fe_xCr_yNi_{1-(x+y)}$, x=0.7−y=0.1, x=0.5−y=0.2, x=0.4−y=0.3, x=0.3−y=0.3, x=0.2−y=0.2, and x=0.1−y=0.2) have been tabulated in Table I. $K\beta$-to-$K\alpha$ x-ray intensity ratios of the elements in alloys are normalized with respect to the values in the case of pure metal. As seen in Table I, the $K\beta$-to-$K\alpha$ x-ray intensity ratio values for 3d metals in alloys are significantly different from those of pure metal. The obtained $K\beta$-to-$K\alpha$ x-ray intensity ratios for pure Fe, Cr, and Ni metals (Table I) are compatible with the results of Raj *et al.* [7], Bhuinya and Padhi [1], Perujo *et al.* [37], and Powłowski *et al.* [5]. Moreover, our present $K\beta$-to-$K\alpha$ x-ray intensity ratio results for Fe and Ni in $Fe_{0,5}Ni_{0,5}$, $Fe_{0,2}Ni_{0,8}$ and for Cr and Ni in $Cr_{0,2}Ni_{0,8}$ alloys are in good agreement with results of Raj *et al.* [7] and Bhuinya and Padhi [1], respectively. Figure 2 is drawn for graphical presentation of values in Table I and shows comparison of the experimental $K\beta$-to-$K\alpha$ x-ray intensity ratios for Fe and Ni in Fe_xNi_{1-x} alloys with the results of MCDF calculations for different valence-electron configurations of Fe and Ni.

3d electron configurations of Fe, Cr, and Ni for various alloys were determined by comparing the experimental values of the $K\beta$-to-$K\alpha$ x-ray intensity ratios with the results of MCDF calculations and the results were given in Table II. Such a comparison provides information about valence-electron configuration of 3d transition metals in alloys and so there is a rearrangement of electrons between 3d and 4s,4p states of individual metal and/or 3d electron transfer between the metal atoms in alloy. Obtained 3d electron populations for pure Fe, Cr, and Ni metals were in agreement with the results of Raj *et al.* [7] (6.93 for Fe and 8.97 for Ni) and Powłowski *et al.* [5] (4.46 for Cr). Changes of 3d electron configurations of Fe, Cr, or Ni in the alloys with respect to pure metals were presented in Table II. Also, number of 3d electrons of Fe and Ni and changes of 3d electrons of Fe and Ni with respect to pure metal were plotted as a function of their own concentrations for Fe_xNi_{1-x} alloys in Figs. 3 and 4, respectively. Changes for some alloys can be easily explained by the rearrangement of electrons between 3d and 4s,4p band states of individual metal atoms. However if 3d electron population changes of Fe, Cr, or Ni in the other alloys (with respect to pure metals) are compared to the corresponding changes for other metal or metals, it indicates that these changes can be explained by assuming the transfer of 3d electrons from atoms of one element to atoms of the other element or elements of alloy.

The approximate numbers of 4s,4p electrons for pure Fe, Cr, and Ni have been obtained by subtracting number of 3d electrons from the total number of valence electrons of the individual atom (eight for Fe, six for Cr, and ten for Ni) and

TABLE II. Evaluated $3d$ electron population values (n_{3d}), total number of $4s,4p$ electrons ($n_{4s,4p}$), and observed change in the number of $3d$ electrons ($\mathcal{C}_{3d}$) with respect to the pure metals for Fe, Cr, and Ni in various alloys.

	Fe			Cr			Ni		
Sample	n_{3d}	$n_{4s.4p}$	$\mathcal{C}_{3d}$	n_{3d}	$n_{4s.4p}$	$\mathcal{C}_{3d}$	n_{3d}	$n_{4s.4p}$	$\mathcal{C}_{3d}$
Pure Fe	7.1491	0.8509							
Pure Cr									
Pure Ni				5.7903	0.2097		9.5218	0.4782	
$Fe_{0.8}Ni_{0.2}$	8.6403	−0.6403	1.4912				7.8594	2.1406	−1.6624
$Fe_{0.7}Ni_{0.3}$	8.2290	−0.2290	1.0799				7.9715	2.0285	−1.5503
$Fe_{0.6}Ni_{0.4}$	7.5605	0.4395	0.4114				8.4202	1.5798	−1.1016
$Fe_{0.5}Ni_{0.5}$	7.1491	0.8509	0.0000				8.3265	1.6735	−1.1953
$Fe_{0.4}Ni_{0.6}$	6.4961	1.5039	−0.6530				8.5162	1.4838	−1.0056
$Fe_{0.3}Ni_{0.7}$	6.3135	1.6865	−0.8356				8.7500	1.2500	−0.7718
$Fe_{0.2}Ni_{0.8}$	5.9727	2.0273	−1.1764				10.000	0.0000	0.4782
$Fe_{0.9}Cr_{0.1}$	7.3470	0.6530	0.4542	4.1447	1.8553	−1.6456			
$Fe_{0.7}Cr_{0.3}$	7.0000	1.0000	0.1072	5.0517	0.9483	−0.7386			
$Fe_{0.5}Cr_{0.5}$	6.6886	1.3114	−0.2042	6.1353	−0.1353	0.3450			
$Cr_{0.2}Ni_{0.8}$				5.1581	0.8419	−0.6322	9.9444	0.0556	0.4226
$Cr_{0.4}Ni_{0.6}$				4.8500	1.1500	−0.9403	8.8209	1.1791	−0.7009
$Cr_{0.5}Ni_{0.5}$				4.3111	1.6889	−1.4792	8.3273	1.6727	−1.1945
$Cr_{0.6}Ni_{0.4}$				3.8422	2.1578	−1.9481	7.8814	2.1186	−1.6404
$Cr_{0.8}Ni_{0.2}$				3.0368	2.9632	−2.7535	6.8831	3.1169	−2.6338
$Fe_{0.7}Cr_{0.1}Ni_{0.2}$	7.3063	0.6937	0.4135	4.3976	1.6024	−1.3927	7.9715	2.0285	−1.0680
$Fe_{0.5}Cr_{0.2}Ni_{0.3}$	7.0000	1.0000	0.1072	5.3805	0.6195	−0.4098	8.5815	1.4185	−0.4580
$Fe_{0.4}Cr_{0.3}Ni_{0.3}$	7.0366	0.9634	0.1438	6.1353	−0.1353	0.3450	9.2087	0.7913	0.1692
$Fe_{0.3}Cr_{0.3}Ni_{0.4}$	6.7218	1.2782	−0.1710	5.8721	0.1279	0.0818	9.0795	0.9205	0.0400
$Fe_{0.2}Cr_{0.2}Ni_{0.6}$	6.1394	1.8606	−0.7534	5.5965	0.4035	−0.1938	9.1615	0.8385	0.1220
$Fe_{0.1}Cr_{0.2}Ni_{0.7}$	5.3177	2.6823	−1.5751	5.1791	0.8209	−0.6112	9.5664	0.4336	0.5269

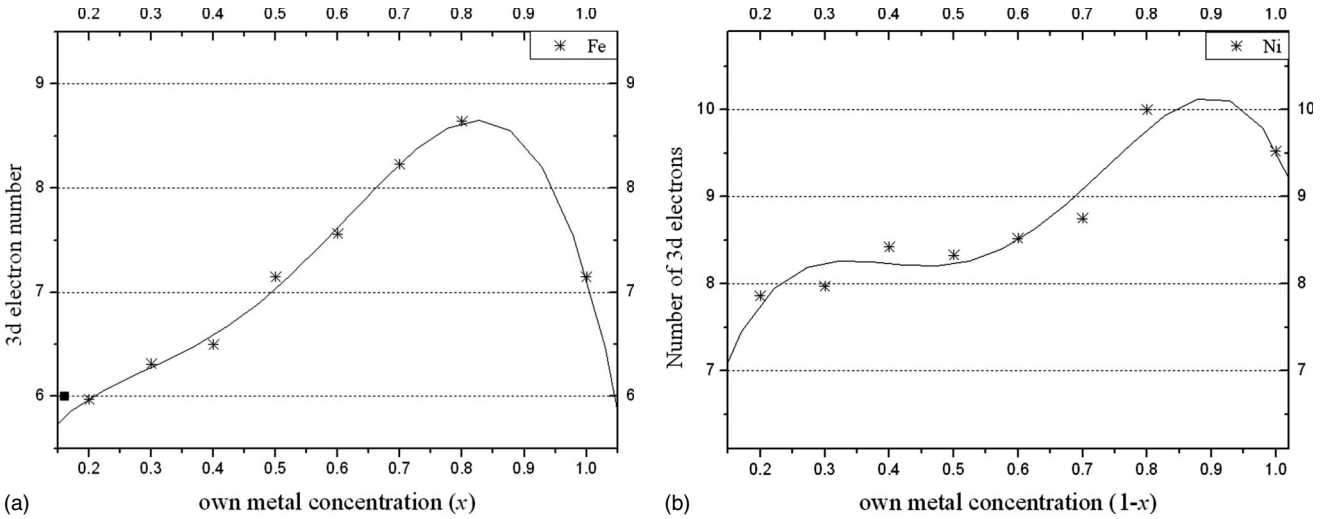

FIG. 3. The number of $3d$ electrons for Fe and Ni as functions of their own concentrations in Fe_xNi_{1-x} alloys.

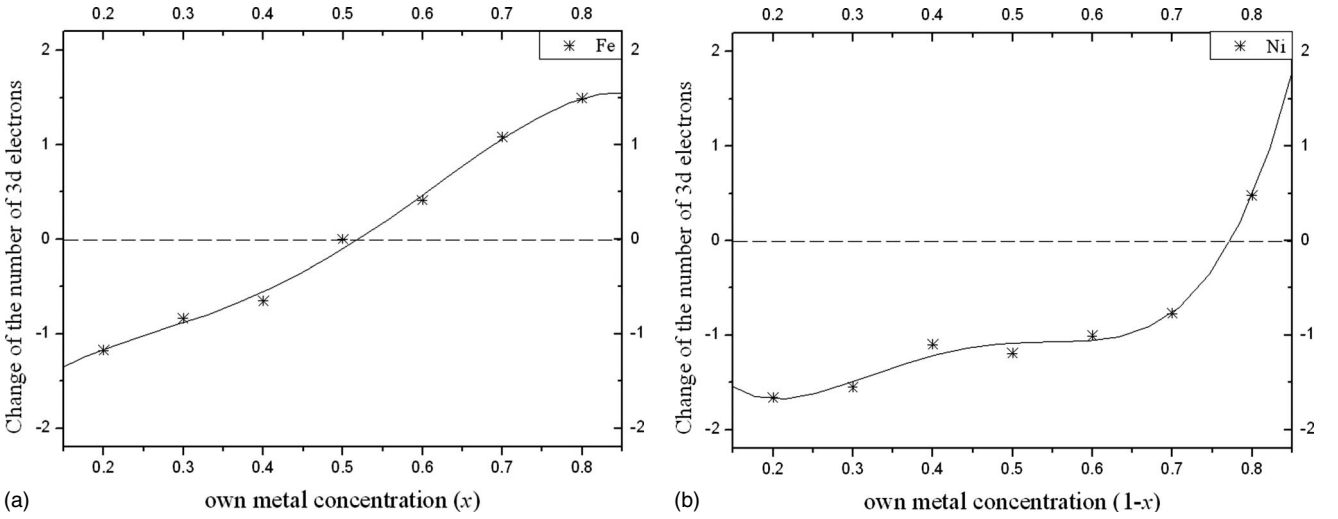

FIG. 4. The changes of the number of 3*d* electrons for Fe and Ni (with respect to pure metals) as functions of their own concentrations in Fe_xNi_{1-x} alloys.

are given in Table II. If Tables I and II are examined together, it is seen that there is a decrease in the measured $K\beta$-to-$K\alpha$ x-ray intensity ratios with increasing 3*d* electron population of the metal in alloys. The change of the number of 3*d* electrons modifies 3*p* orbitals much stronger than 2*p* orbitals, so main modifications are seen in $K\beta$ transitions and almost there is no modification in $K\alpha$ transitions. This causes changing in the $K\beta$-to-$K\alpha$ x-ray intensity ratio.

It can be seen from Table II that for some alloys in the same group, delocalization and charge transfer phenomena are opposite directions and larger than the others, so valence-electron configurations for these alloys are different. The differences in valence-electron configuration of these alloys can cause different and special physical properties (such as high permeability, small magnetostriction, low coercivity, and other magnetic properties) from the other alloys. For example, $Fe_{0.2}Ni_{0.8}$ is a special alloy with very good magnetic properties and has large application scale [38]. For $Fe_{0.2}Ni_{0.8}$ alloy the obtained average number of 3*d* electrons is more than the number calculated with superposition method and the 4*s*,4*p* orbitals are also almost empty (Table III). Already $K\beta$-to-$K\alpha$ x-ray intensity ratios of this alloy are different from the alloys of same group.

After all we calculated numbers of 3*d* and 4*s*,4*p* electrons for each alloy with weighted average and superposition. Superposition values of each alloys are calculated with using numbers of 3*d* and 4*s*,4*p* electrons of relevant pure metals. The results are shown in Table III. It can be seen from the table that for all studied alloys these superposition numbers are different from the weighted average numbers of 3*d* and 4*s*,4*p* electrons.

IV. CONCLUSION

In this paper, it is shown that the $K\beta$-to-$K\alpha$ x-ray intensity ratios can be used as a sensitive tool to determine the valence-electron configurations of 3*d*-transition metals in alloys. The valence-electron configurations of 3*d*-transition metals in the alloys may be evaluated by comparing the measured $K\beta$-to-$K\alpha$ x-ray intensity ratios to the results of multiconfiguration Dirac-Fock calculations. The obtained valence-electron populations of 3*d* transition metals for vari-

TABLE III. Comparison of estimated weighted average number of 3*d* and 4*s*,4*p* electrons ($\mathcal{A}_{3d}$ and $\mathcal{A}_{4s,4p}$) for various alloys with the superposition values of 3*d* and 4*s*,4*p* electrons ($\mathcal{S}_{3d}$ and $\mathcal{S}_{4s,4p}$) obtained from the pure metal values.

Sample	$\mathcal{A}_{3d}$	$\mathcal{S}_{3d}$	$\mathcal{A}_{4s,4p}$	$\mathcal{S}_{4s,4p}$
$Fe_{0.8}Ni_{0.2}$	8.4841	7.6236	0.0841	0.7764
$Fe_{0.7}Ni_{0.3}$	8.1518	7.8609	0.4483	0.7391
$Fe_{0.6}Ni_{0.4}$	7.9044	8.0982	0.8956	0.7018
$Fe_{0.5}Ni_{0.5}$	7.7378	8.3355	1.2622	0.6646
$Fe_{0.4}Ni_{0.6}$	7.7082	8.5727	1.4918	0.6273
$Fe_{0.3}Ni_{0.7}$	8.0191	8.8100	1.3810	0.5900
$Fe_{0.2}Ni_{0.8}$	9.1945	9.0472	0.4055	0.5527
$Fe_{0.9}Cr_{0.1}$	7.0268	6.7826	0.7014	1.0175
$Fe_{0.7}Cr_{0.3}$	6.4155	5.6660	0.9845	0.8380
$Fe_{0.5}Cr_{0.5}$	6.4120	6.3416	0.5881	0.6585
$Ni_{0.8}Cr_{0.2}$	8.9871	8.4225	0.2129	0.7781
$Ni_{0.6}Cr_{0.4}$	7.2325	7.4593	1.1675	0.9419
$Ni_{0.5}Cr_{0.5}$	6.3192	6.9778	1.6808	1.0238
$Ni_{0.4}Cr_{0.6}$	5.4579	6.4962	2.1421	1.1056
$Ni_{0.2}Cr_{0.8}$	3.8061	5.5330	2.9939	1.2694
$Fe_{0.7}Cr_{0.1}Ni_{0.2}$	7.1485	7.2119	1.0515	0.9881
$Fe_{0.5}Cr_{0.2}Ni_{0.3}$	7.1506	7.3163	1.0495	0.8837
$Fe_{0.4}Cr_{0.3}Ni_{0.3}$	7.4178	7.2061	0.5822	0.7939
$Fe_{0.3}Cr_{0.3}Ni_{0.4}$	7.4100	7.4207	0.7900	0.7793
$Fe_{0.2}Cr_{0.2}Ni_{0.6}$	7.8441	7.9603	0.9559	0.8397
$Fe_{0.1}Cr_{0.2}Ni_{0.7}$	8.2641	8.1750	0.7359	0.8250

ous alloy compositions are different. The observed significant changes in the 3*d* electron population of 3*d* transition metals in various alloy with respect to the pure metal arise from delocalization and/or charge transfer. In other words, to reliably explain evaluated changes of the 3*d* electron population for 3*d* transition metals in their alloys, it is necessary to take into account the rearrangement of electrons between 3*d* and 4*s*,4*p* states of metal atoms and the transfer of 3*d* electrons between elements. The results of this study will help us to understand how $K\beta$-to-$K\alpha$ x-ray intensity ratios depend on the valence-electron configurations of 3*d* transition metals for different alloy compositions.

[1] C. R. Bhuinya and H. C. Padhi, J. Phys. B **25**, 5283 (1992).
[2] C. R. Bhuinya and H. C. Padhi, Phys. Rev. A **47**, 4885 (1993).
[3] H. C. Padhi and B. B. Dhal, Solid State Commun. **96**, 171 (1995).
[4] S. Raj, H. C. Padhi, and M. Polasik, Nucl. Instrum. Methods Phys. Res. B **155**, 143 (1999).
[5] F. Pawłowski, M. Polasik, S. Raj, H. C. Padhi, and D. K. Basa, Nucl. Instrum. Methods Phys. Res. B **195**, 367 (2002).
[6] S. Raj, H. C. Padhia, M. Polasik, F. Pawłowski, and D. K. Basa, Solid State Commun. **116**, 563 (2000).
[7] S. Raj, H. C. Padhi, M. Polasik, F. Pawłowski, and D. K. Basa, Phys. Rev. B **63**, 073109 (2001).
[8] G. Brunner, M. Nagel, E. Hartmann, and E. Arndt, J. Phys. B **15**, 4517 (1982).
[9] T. Mukoyama, K. Taniguchi, and H. Adachi, Phys. Rev. B **34**, 3710 (1986).
[10] A. Kucukonder, Y. Sahin, E. Buyyukkasap, and A. Kopya, J. Phys. B **26**, 101 (1993).
[11] H. C. Padhi, C. R. Bhuinya, and B. B. Dhal, J. Phys. B **26**, 4465 (1993).
[12] C. N. Chang, S. K. Chiou, and C. L. Luo, Solid State Commun. **87**, 987 (1993).
[13] C. N. Chang, C. Chen, C. C. Yen, Y. H. Wu, C. W. Wu, and S. K. Choi, J. Phys. B **27**, 5251 (1994).
[14] E. Arndt, G. Brunner, and E. Hartmann, J. Phys. B **15**, L887 (1982).
[15] S. Raj, B. B. Dhal, H. C. Padhi, and M. Polasik, Phys. Rev. B **58**, 9025 (1998).
[16] S. Raj, B. B. Dhal, H. C. Padhi, and M. Polasik, Nucl. Instrum. Methods Phys. Res. B **145**, 485 (1998).
[17] S. Raj, H. C. Padhi, M. Polasik, and D. K. Basa, Solid State Commun. **110**, 275 (1999).
[18] S. Raj, H. C. Padhi, D. K. Basa, M. Polasik, and F. Pawłowski, Nucl. Instrum. Methods Phys. Res. B **152**, 417 (1999).
[19] S. Raj, H. C. Padhi, and M. Polasik, Nucl. Instrum. Methods Phys. Res. B **160**, 443 (2000).
[20] S. Raj, H. C. Padhi, P. Rayachaudhury, A. K. Nigam, R. Pinto, M. Polasik, and F. Pawłowski, Nucl. Instrum. Methods Phys. Res. B **174**, 344 (2001).
[21] S. Raj, H. C. Padhi, P. Palit, D. K. Basa, M. Polasik, and F. Pawłowski, Phys. Rev. B **65**, 193105 (2002).
[22] M. Polasik, Phys. Rev. A **58**, 1840 (1998).
[23] T. Mukoyama, K. Taniguchi, and H. Adachi, X-Ray Spectrom. **29**, 426 (2000).
[24] I. P. Grant, B. J. McKenzie, P. H. Norrington, D. F. Mayers, and N. C. Pyper, Comput. Phys. Commun. **21**, 207 (1980).
[25] B. J. McKenzie, I. P. Grant, and P. H. Norrington, Comput. Phys. Commun. **21**, 233 (1980).
[26] I. P. Grant, J. Phys. B **7**, 1458 (1974).
[27] J. Hata and I. P. Grant, J. Phys. B **16**, 3713 (1983).
[28] I. P. Grant and B. J. McKenzie, J. Phys. B **13**, 2671 (1980).
[29] I. P. Grant, Int. J. Quantum Chem. **25**, 23 (1984).
[30] I. P. Grant, Adv. Phys. **19**, 747 (1970).
[31] K. G. Dyall, I. P. Grant, C. T. Johnson, F. A. Parpia, and E. P. Plummer, Comput. Phys. Commun. **55**, 425 (1989).
[32] I. Han, M. Sahin, L. Demir, and Y. Sahin, Appl. Radiat. Isot. **65**, 669 (2007).
[33] I. Han, L. Demir, and M. Agbaba, Radiat. Phys. Chem. **76**, 1551 (2007).
[34] L. Gerward, N. Guilbert, K. B. Jensen, and H. Levring, Radiat. Phys. Chem. **60**, 23 (2001).
[35] L. Gerward, N. Guilbert, K. B. Jensen, and H. Levring, Radiat. Phys. Chem. **71**, 653 (2004).
[36] D. F. Jackson and D. J. Hawkes, Phys. Rep. **70**, 169 (1981).
[37] A. Perujo, J. A. Maxwell, W. J. Teesdale, and J. L. Campbell, J. Phys. B **20**, 4973 (1987).
[38] B. Nadgorny, R. J. Soulen, Jr., M. S. Osofsky, I. I. Magin, G. Laprade, R. J. M. Van de Veerdonk, A. A. Smits, S. F. Chen, E. F. Skelton, and S. B. Qadri, Phys. Rev. B **61**, R3788 (2000).